10204 *Macromolecules* **2010**, *43*, 10204–10207
DOI: 10.1021/ma102268b

Macromolecules
COMMUNICATION TO THE EDITOR

Generalized Force−Extension Relation for Wormlike Chains in Slit Confinement

Yeng-Long Chen,* Po-keng Lin, and Chia-Fu Chou

Institute of Physics and Research Center for Applied Sciences, Academia Sinica, Nangang, Taipei 11529, Taiwan

Received October 4, 2010
Revised Manuscript Received November 29, 2010

DNA dynamics in strongly confined environments has many implications for biological mechanisms, including nucleosome formation, DNA translocation across a membrane, and virus DNA packaging. Fundamental questions about how DNA inherent rigidity affects its functions and interactions with proteins to be clarified.[1−5] The conformation and dynamics of semiflexible chains (SFC) such as DNA depend strongly on the molecular entropy contributions from temperature and confinement, inherent molecular stiffness, and external forces such as flow and electric field. In recent years, advances in nanofabrication has greatly facilitated extensive single DNA studies in well-defined nanoslits and nanochannels and allowed direct probing of single DNA molecule dynamics.[6−12] These novel experimental measurements have verified numerous theoretical predictions of polymer dynamics in free solution and in confinement. In particular, the conformation and dynamics of SFC in subpersistence length confinement is found to be qualitatively different than unconfined SFC.

Insights into the dynamics of confined DNA molecules may be gained by understanding the entropic elasticity of DNA. This relation between the force (f) required to stretch a DNA molecule to a given extension (X), defined as the maximum length of the molecule, has been experimentally measured by optical tweezers in free solution.[13,14] In channels where the height (H) is comparable to the SFC radius of gyration (R_g), a force−extension relation ($f-X$) has been developed by considering the classic "blob chain" model.[15] In smaller channels where H is comparable to the chain persistence length P, the concept of the "deflected segment length" for the SFC segmental correlation length in strong confinement has been well developed by Odijk and others.[16−22] For $H < P$, a qualitative change to DNA conformation and relaxation dynamics occurs due to confinement-induced change in the segmental correlation length l_c, which separates into longitudinal ($l_\parallel$) and transversal ($l_\perp$) components in the unconfined and confined dimensions, as shown in Figure 1. In square nanochannel confinement, $l_\perp$ is proportional to H, and $l_\parallel$ can be comparable to the chain contour length L.[23] This has been confirmed by recent studies in nanofluidic devices with dimensions smaller than 100 nm. The studies found that for DNA confined in nanochannels or nanoslits smaller than the Kuhn correlation length $\sigma_k \approx 100$ nm[7,24] the chain relaxation time decreases as the channel height decreases, which is opposite to the trend when chains are confined in channels larger than σ_k.[25−28] However, there is a distinction between channels, in which the chains are strongly confined by four walls, and slits, in which the chains are strongly confined by two walls. In small channels, coordinated chain rotation is strongly hindered, whereas chains undergo rotational relaxation in slits.[6] In this Communication, we investigate how strong confinement affects the segmental correlation length and employ the relation between $l_\parallel$ and H to formulate a force−extension relation for strongly confined SFC.

DNA conformation and dynamics in confinement, in flow, and under external fields depends on the balance between entropy, elasticity, and external force fields. Much progress has been made in the direct measurements of DNA elasticity using optical and magnetic tweezers.[13,14,29] The exact and approximate form of the $f-x$ relation, where $x = X/L$ is the relative extension, for long ($L \gg P$) DNA molecules has been derived by Marko and Siggia,[13] with the approximate form given by

$$\frac{fP}{k_BT} = \frac{1}{4}\left[\frac{1}{(1-x)^2} - 1\right] + x \tag{1}$$

where k_BT is the thermal energy. In the $x \to 0$ limit, the chain elastic force is purely entropic and varies linearly with x and k_BT/P, which may be considered as the entropic energy of a chain with L/P statistically independent segments. As $x \to 1$, the stretching force is highly nonlinear and depends on the inherent stiffness of the DNA molecule. This wormlike chain (WLC) elastic spring force relation has served as the mechanical basis for coarse-grained DNA bead−spring models for studying DNA conformation and dynamic properties in flow and in electric fields. However, for a DNA molecule with a finite length at nonzero temperature, the equilibrium relative extension x_0 is nonzero with $f = 0$ due to thermal fluctuations, and eq 1 requires a correction. x_0 depends on L, P, H, and the intrachain excluded volume interactions. The intrachain excluded volume interactions may be characterized by the parameter $Z = 2\pi L^2\sigma/P^3$ in free solution, where σ is the segment width.[30,31] For $Z < 1$, the chains follow ideal random walk statistics. For $Z > 1$, the chains are self-avoiding walks with $x_0 \sim L^{-0.4}$ and becomes negligible for large L (e.g., $x_0 \approx 0.05$ for λ-DNA).[32] In slit confinement, $Z = L\sigma/PH$, and strong intrachain excluded volume interactions lead to significant x_0 under strong confinement.[33] Thus, the force for small extension may be included by considering a linear force dependence on the perturbation from a finite x_0. In addition, the entropic energy of the chain is reduced due to the reduction of statistically independent chain segments as the segmental correlation length increases. Thus, $f \sim (x - x_0)(k_BT/l_\parallel)$ for $x \sim x_0$. At larger chain extension, the influence of confinement is expected to be negligible due to reduced transversal chain fluctuations, and the Marko−Siggia force−extension relation would be recovered. A modified WLC can thus be written as

$$\frac{fl_\parallel}{k_BT} = \frac{1}{4}\left[\frac{1}{(1-x)^2} - \frac{1}{(1-x_0)^2}\right] + (x - x_0) \tag{2}$$

where it satisfies the limit that $f = 0$ at $x = x_0$. In strong confinement, the entropic spring constant $k_BT/l_\parallel$ replaces k_BT/P as the chain stiffness in the longitudinal (unconfined) axis. The longitudinal correlation length $l_\parallel$ can be determined from simulations of the conformation of confined SFC.

Equation 2 is verified by performing Brownian dynamics simulations of strongly confined SFC. A SFC is modeled as a N-spring chain, each spring with a unit length σ_m. All lengths are reported in units of σ_m. The conformation and dynamics of SFC

*Corresponding author. E-mail: yenglong@phys.sinica.edu.tw.

 Published on Web 12/07/2010

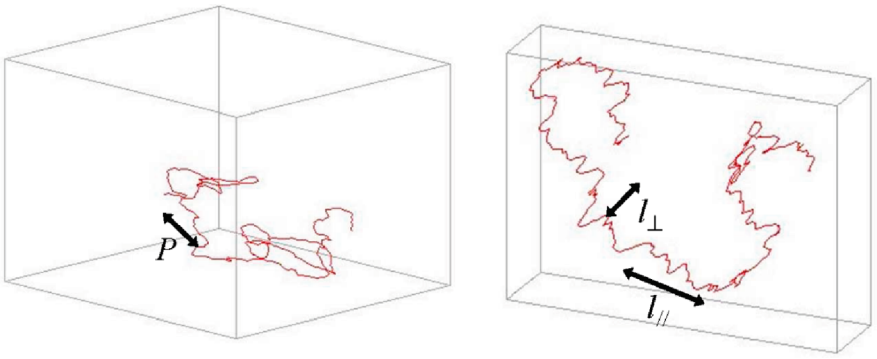

Figure 1. (left) Weakly confined chain with $L = 400$, $K_B = 6.6$, $H = 60$. (right) Strongly confined chain with $L = 400$, $K_B = 5$, $H = 5$. K_B is the bending modulus of the chain (see text).

of lengths $L = 400$, 800, and 1600 with $P = 5$, 6.6, 10, 13.2, 20, and 40 are examined. The harmonic spring potential energy is

$$\frac{U_{\text{spring}}}{k_B T} = \frac{k_v}{2{\sigma_m}^2}\sum_i (|\mathbf{r}_i - \mathbf{r}_{i+1}| - \sigma_m)^2 \quad (3)$$

with $k_v = 400$ and $k_B T = 1$. $\mathbf{r}_i$ is the position of the ith bead of the chain. The beads repel each other with the repulsive part of the Morse potential with a cutoff distance of $1.5\sigma_m$

$$U_{M,\text{rep}} = \varepsilon_m k_B T \sum_{i,j,i<j} \exp[-\alpha_m(r_{i,j} - \sigma_m)] \quad (4)$$

with $\varepsilon_m = 6$, $\alpha_m = 24$ chosen to give a hard repulsive core for the beads. $r_{i,j}$ is the distance between the ith and jth beads. The chain rigidity is introduced by a bending potential of the angle between segments $\mathbf{v}_{i-1} = (\mathbf{r}_{i-1} - \mathbf{r}_i)$ and $\mathbf{v}_i = (\mathbf{r}_i - \mathbf{r}_{i+1})$, given by

$$U_{\text{bend}} = K_B k_B T \sum_i \left(1 - \frac{(\mathbf{r}_{i-1} - \mathbf{r}_i)(\mathbf{r}_i - \mathbf{r}_{i+1})}{|\mathbf{r}_{i-1} - \mathbf{r}_i||\mathbf{r}_i - \mathbf{r}_{i+1}|}\right) \quad (5)$$

The bending modulus K_B determines the persistence length P, which is measured from the exponential decay length of the correlation function $C(|i-j|) = \langle \mathbf{v}_i \cdot \mathbf{v}_{i+j} \rangle$. In these studies, $P \approx K_B$. The repulsive interaction between the polymer and the walls are modeled by a cubic potential with a range of σ_m.[34] An overdamped Langevin equation[35−37] with freely draining hydrodynamic interactions propagates the monomer trajectory, given by

$$-\zeta\frac{d\mathbf{r}_i}{dt} + \mathbf{f}_i^R(t) - \frac{\partial U}{\partial \mathbf{r}_i} = 0 \quad (6)$$

$\zeta = 3\pi\eta\sigma_m$ is the friction coefficient of a bead, and η is the solvent viscosity. The thermal fluctuation force $\mathbf{f}_i^R(t)$ has a Gaussian distribution with zero mean and a variance $2k_B T\zeta/\Delta\tau$ that satisfies the fluctuation−dissipation theorem. The internal forces are given by $(-\partial U/\partial \mathbf{r}_i)$. The integration time step is $\Delta t = 10^{-2}\tau_m$, where $\tau_m = \zeta{\sigma_m}^2/k_B T$ is the bead diffusion time. Chain dynamics are first equilibrated for 10^8−10^9 time steps. Statistics of the segmental correlation length are collected for 20−40 chains for more than 20 chain relaxation times. The chain force−extension relation is determined by applying equal and opposite forces on the opposite chain ends and measuring the steady-state average chain extension at the given force.

The chains are first equilibrated for a given confinement geometry, and the confinement effects on the chain conformation are characterized by determining the chain segmental correlation length l_c. $l_\parallel$ and $l_\perp$ are determined from the exponential decay length of the segmental correlation function $C(|i-j|)$, as shown in the Figure 2 insets. Even in a very small slit, the longitudinal segment−segmental correlation would decay to zero for sufficiently long segment length due to the ability of chain segments to rotate and relax in the slit.

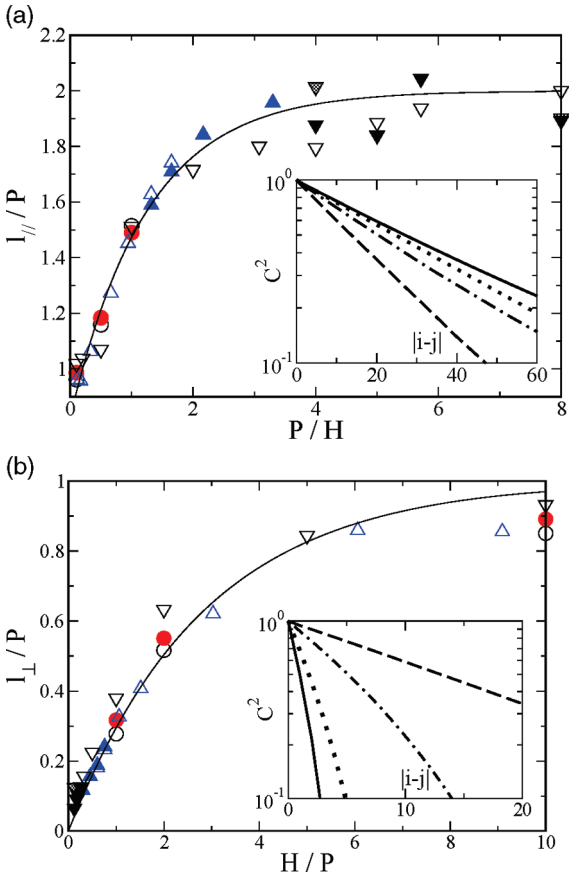

Figure 2. Chain longitudinal (a) and transverse (b) segmental correlation length ratio as a function of the confinement ratio for $L/P = 80$ (circle) and $P = 5$ (empty) and 10 (solid). $L/P = 60.6$ (triangle), $P = 6.6$ (empty), and 13.2 (solid). $L/P = 10$ (downward triangle), $L = 400$ (empty), 600 (shaded), and 800 (solid). The solid line shows the best fit. Inset: segmental correlation function for $L = 400$, $P = 40$, $H = 5$ (solid), 10 (dotted), 20 (dot-dashed), and 400 (dashed).

As the slit height decreases, Figure 2a shows that for very weak confinement $P < H < R_g$, $l_\parallel = P$ as expected. The ratio between the segmental correlation length and P is shown to collapse for various L and P for a given P/H. Thus, $l_\parallel/P$ is independent of L for sufficiently long chains ($L/P > 10$), and it depends only on P/H. The collapse of $l_\parallel/P$ for the wide range of L and P examined also indicates that these systems may be generalized to the long

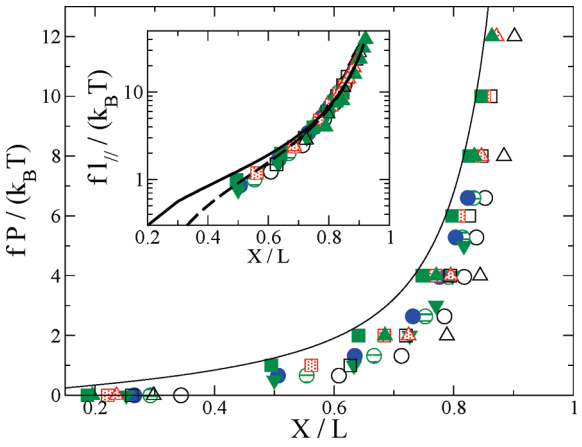

Figure 3. Force−relative extension relation of SFC in slit. $L/P = 60.6$, $P/H = 0.75$ (empty circle), 1.05 (lined circle), 1.5 (solid circle). $L/P = 80$, $P = 10$, $H = 10$ (empty square), 20 (shaded square), 100 (solid square). $P = 20$, $H = 5$ (empty triangle), 20 (shaded triangle), 40 (solid triangle). $L/P = 160$, $P = 5$, $H = 5$ (solid downward triangle). The solid line is eq 1. Inset: rescaled force−relative extension relation of SFC in slit. The solid line is eq 1, and the dashed line is eq 2.

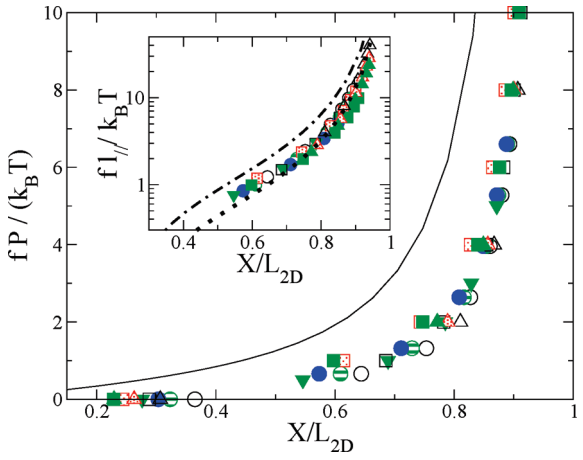

Figure 4. Force−projected relative extension relation of SFC in slit. $L/P = 60.6$, $P/H = 0.75$ (empty circle), 1.05 (lined circle), 1.5 (solid circle). $L/P = 80$, $P = 10$, $H = 10$ (empty square), 20 (shaded square), 100 (solid square). $P = 20$, $H = 5$ (empty triangle), 20 (shaded triangle), 40 (solid triangle). $L/P = 160$, $P = 5$, $H = 5$ (solid downward triangle). The solid line shows eq 1. Inset: rescaled force−projected relative extension relation of SFC in slit. The dot-dashed line is eq 2, and the dotted line is the halved force of eq 2.

chain behavior. For moderate confinement ($0.2 < P/H < 2$), $l_{\parallel}/P$ grows linearly with P/H with a slope of ~0.8. As the confinement effect increases ($P/H > 2$), $l_{\parallel}/P$ grows and saturates near the value of 2. The curve $l_{\parallel}/P = 2 - \exp[-0.8(P/H - 0.2)]$ fits the growth of $l_{\parallel}/P$ for $P/H > 0.2$. For $P/H < 0.2$, $l_{\parallel}/P = 1$. For large P/H, larger variation between chains with different P is due to the differences in H for given P/H, and it may be attributed to the finite size excluded volume interactions and packing effects between the beads and the wall. It is expected the results would converge for $H/\sigma_m \gg 1$. This may be attributed to the ability of the chain segments to perform random walks in two dimensions, thus relaxing the intersegmental correlation. In contrast, in strong quasi-one-dimensional confinement, the chain segments may not undergo one-dimensional random walk due to intersegmental excluded volume interactions, and the segmental correlation function does not relax in very small square channels.[23]

In contrast to $l_{\parallel}$, the transverse segmental correlation length $l_{\perp}$ decreases as the slit height decreases. Figure 2b shows $l_{\perp}/P$ is linearly dependent on H/P for $H/P < 2$. As H further increases, $l_{\perp}$ approaches P as expected. The inset of Figure 2b shows that the transverse correlation function decreases as H decreases and enters the chain deflection regime for $H/P < 1$. The curve $l_{\perp}/P = 1 - \exp[-0.35H/P]$ is found to best fit the results for $l_{\perp}/P$, and it gives $l_{\perp} = 0.35H$ for small H/P. The linear dependence of $l_{\perp}$ on H is predicted for wormlike chains confined in square channels,[18] which suggests that the magnitude of the fluctuations in the confined dimension are similar in slit and square confinement. The linear dependence also agrees with experimental studies that have shown the chain extensional relaxation time depends on H^2 for $H/P < 2$.[7]

The increase of the longitudinal correlation length as H decreases affects the force−extension relation for strongly confined chains. Whether eq 2 captures this change is further investigated by modeling chain stretching under external force. The SFC is stretched by pulling the chain ends in opposite directions with equal force. The average chain extension at a constant force is measured. Figure 3 shows that as H decreases, the force required to stretch the chain decreases. This corresponds to more swollen chains at smaller H, and the smaller force needed to stretch an already more swollen chain. The L-independence (long chain) is verified, as seen in the collapse of the $f-x$ curve of $L/P = 80$ and 160 at $H/P = 1$. The P-independence (long persistence length segment) is also verified, as seen in the collapse of the $f-x$ curves of $P = 10$ and 20 at $L/P = 80$ for $H/P = 1$ and 2. It can be observed that eq 1 captures the $f-x$ relation at high x for $H/P \gg 1$ but overpredicts the extensional force for moderately and strongly confined chains. For all chain length and confinement, the equilibrium chain extension x_0 depends on both L/P and H/P. However, at high relative chain extension, the extension force depends only on H/P and may be rescaled by the entropic energy of a longitudinally correlated segment $k_BT/l_{\parallel}$. Figure 3 inset shows that the $f-x$ curves for various L/P and H/P collapse onto eq 2 for $fl_{\parallel}/k_BT > 1$, when the extensional force is properly scaled. For $fl_{\parallel}/k_BT < 1$, it is found that eq 1 does not capture the behavior near $x = x_0$, as expected. Instead, $fl_{\parallel}/k_BT = (x - x_0)$ is found for various $x_0(L/P,H/P)$.

In order to make direct comparisons to experiments, the differences between the theoretical results and the experiments must be reconciled. Microscopy observations of DNA conformation are unable to measure the relative chain extension x if the chain contour length is not known *a priori* due to the limitation that the observed image is the two-dimensional projection of the chain. However, simulations may be employed to determine both the two- and three-dimensional chain contour length and extension, and the force−extension relation from the simulations may thus be useful for determining the external forces acting on a stretched DNA molecule.

Figure 4 shows the measured relative projected chain extension $x_p = X_p/L_{2D}$, where X_p and L_{2D} are the projected chain extension and contour length that can be measured by microscopy, at a given extensional force. As found in the $f-x$ relation, there are significant differences between the extensional forces of chains with different L/P and H/P. Qualitatively, the extensional force decreases as H decreases, as found in the $f-x$ relation. Unsurprisingly, eq 1 overestimates the extensional force for all H, since in free solution one would expect L_{2D} to be smaller than L. Analogous to the $f-x$ relation, rescaling the force by $fl_{\parallel}/k_BT$ collapses the $f-x_p$ curves for various L/P and H/P, as shown in the Figure 4 inset. It is found that eq 2 also overestimates the scaled extensional force significantly. Interestingly, it is empirically found that reducing the extensional force of eq 2 by a factor of 2 would quantitatively agree with the collapsed data for $fl_{\parallel}/k_BT > 1$. This suggests that a simple $f-x_p$ relation exists that can be applied to directly determine the extensional force acting on a DNA molecule from its average projected extension.

This work has investigated how strong slit confinement affects the bending rigidity of long semiflexible chains and changes the segmental correlation length. It is found that as the slit height becomes smaller than the chain persistence length, the isotropic symmetry of the segmental correlation length is broken into longitudinal and transverse components. An analogy to the dynamics for polymers in dense entangled melt may be considered, where polymers are under tubelike confinement (transverse) and undergo snakelike reptation motion along the chain backbone (longitudinal). Furthermore, the force−extension relation of highly confined semiflexible chains is measured, and it is found to validate the modified wormlike chain formula of eq 2. The significance of this finding is that the entropic energy of confined chain segments is determined by the segmental correlation length for a given confinement instead of the chain persistence length. This generalized force−extension relation may be applied to directly determine the external forces exerted on a chain, such as DNA molecules extended by entropic traps such as nano/microchannels interfaces, and energetic traps such as attractive membranes and surfaces. For SFC molecules of unknown size, the results in this study also show that the measured projected contour length may be employed to determine the contour length, given that the ratio between the slit height and the persistence length is known. Moreover, coarse-grained models for slit-confined DNA may use the dumbbell model with the modified wormlike chain spring law here to help further understanding of strongly confined or adsorbed DNA dynamics. Future studies will address how these conformational changes affect chain relaxation and chain dynamics inside slit and square channels.

Acknowledgment. We acknowledge financial support from Academia Sinica Research Program on Nanoscience and Nanotechnology, Academia Sinica Foresight Project (97-M02) to C.F. Chou, and National Science Council of ROC to Y.-L. Chen (98-2112-M-001-004-MY3) and C.F. Chou (96-2112-M-001-024-MY3 and 99-2112-M-001-027-MY3).

References and Notes

(1) Sauer, M.; Angerer, B.; Ankenbauer, W.; Földes-Papp, Z.; Göbel, F.; Han, K.-T.; Rigler, R.; Schulz, A.; Wolfrum, J.; Zander, C. *J. Biotechnol.* **2001**, *86*, 181.
(2) Tegeneldt, J. O.; Prinz, C.; Cao, H.; Huang, R. L.; Austin, R. H.; Chou, S. Y.; Cox, E. C.; Sturm, J. C. *Anal. Bioanal. Chem.* **2004**, *378*, 1678.
(3) Perkins, T. T.; Quake, S. R.; Smith, D. E.; Chu, S. *Science* **1994**, *264*, 822.
(4) Smith, D. E.; Perkins, T. T.; Chu, S. *Phys. Rev. Lett.* **1995**, *75*, 4146.
(5) Turner, S. W. P.; Cabodi, M.; Craighead, H. G. *Phys. Rev. Lett.* **2002**, *88*, 128103.
(6) Hsieh, C.-C.; Balducci, A.; Doyle, P. S. *Macromolecules* **2007**, *40*, 5196.
(7) Reisner, W.; Morton, K. J.; Riehn, R.; Wang, Y. M.; Yu, Z.; Rosen, M.; Sturm, J. C.; Chou, S. Y.; Frey, E.; Austin, R. H. *Phys. Rev. Lett.* **2005**, *94*, 196101.
(8) Strychalski, E. A.; Levy, S. L.; Craighead, H. G. *Macromolecules* **2008**, *41*, 7716.
(9) Reisner, W.; Larsen, N. B.; Silahtaroglu, A.; Kristensen, A.; Tommerup, N.; Tegenfeldt, J. O.; Flyvbjerg, H. *Proc. Natl. Acad. Sci. U.S.A* **2010**, *107*, 13294.
(10) Reisner, W.; Larsen, N. B.; Flyvbjerg, H.; Tegenfeldt, J. O.; Kristensen, A. *Proc. Natl. Acad. Sci. U.S.A* **2009**, *106*, 79.
(11) Del Bonis-O'Donnell, J. T.; Reisner, W.; Stein, D. *New J. Phys.* **2009**, *11*.
(12) Guo, L. J.; Cheng, X.; Chou, C. F. *Nano Lett.* **2004**, *4*, 69.
(13) Marko, J. F.; Siggia, E. D. *Macromolecules* **1994**, *28*, 8759.
(14) Perkins, T. T.; Quake, S. R.; Smith, D. E.; Chu, S. *Science* **1994**, *264*, 822.
(15) Tang, J.; Trahan, D. W.; Doyle, P. S. *Macromolecules* **2010**, *43*, 3081.
(16) Burkhardt, T. *J. Phys. A: Gen. Phys.* **1995**, *28*, L629.
(17) Burkhardt, T. *J. Phys. A: Gen. Phys.* **1997**, *30*, L167.
(18) Odijk, T. *Macromolecules* **1983**, *16*, 1340.
(19) Odijk, T. *J. Chem. Phys.* **2006**, *125*, 204904.
(20) Cifra, P. *J. Chem. Phys.* **2009**, *131*, 224903.
(21) Cifra, P.; Benkova, Z.; Bleha, T. *J. Phys. Chem. B* **2009**, *113*, 1843.
(22) Jo, K.; Dhingra, D. M.; Odijk, T.; De Pablo, J. J.; Graham, M. D.; Runnheim, R.; Forrest, D.; Schwartz, D. C. *Proc. Natl. Acad. Sci. U.S.A* **2007**, *104*, 2673.
(23) Cifra, P.; Benkova, Z.; Bleha, T. *Phys. Chem. Chem. Phys.* **2010**, *12*, 8934.
(24) Bonthuis, D. J.; Meyer, C.; Stein, D.; Dekker, C. *Phys. Rev. Lett.* **2008**, *101*, 108303.
(25) Brochard, F.; de Gennes, P. G. *J. Chem. Phys.* **1977**, *67*, 52.
(26) Lin, P.-K.; Fu, C.-C.; Chen, Y.-L.; Chen, Y.-R.; Wei, P.-K.; Kuan, C. H.; Fann, W. S. *Phys. Rev. E* **2007**, *76*, 011806.
(27) Balducci, A.; Mao, P.; Han, J.; Doyle, P. S. *Macromolecules* **2006**, *39*, 6273.
(28) Lin, P.-K.; Lin, K.-H.; Fu, C.-C.; Lee, K.-C.; Wei, P.-K.; Pai, W.-W.; Tsao, P.-H.; Chen, Y.-L.; Fann, W. S. *Macromolecules* **2009**, *42*, 1770.
(29) Bustamante, C.; Bryant, Z.; Smith, S. B. *Nature* **2003**, *421*, 423.
(30) Yamakawa, H.; Stockmayer, W. H. *J. Chem. Phys.* **1972**, *57*, 2843.
(31) Moon, J.; Nakanishi, H. *Phys. Rev. A* **1991**, *44*, 6427.
(32) Doi, M.; Edwards, S. F. *Theory of Polymer Dynamics*; Oxford University Press: Oxford, 1986.
(33) Odijk, T. *Phys. Rev. E* **2008**, *77*, 060901(R).
(34) Jendrejack, R. M.; Schwartz, D. C.; Graham, M. D.; de Pablo, J. J. *J. Chem. Phys.* **2003**, *119*, 1165.
(35) Ermak, D. L.; McCammon, J. A. *J. Chem. Phys.* **1978**, *69*, 1352.
(36) Beard, D. A.; Schlick, T. *J. Chem. Phys.* **2000**, *112*, 7313.
(37) Sakaue, T.; Yoshikawa, K.; Yoshimura, S. H.; Takeyasu, K. *Phys. Rev. Lett.* **2001**, *87*, 078105.